

Faraday patterns in dipolar Bose-Einstein condensates

R. Nath and L. Santos

Institut für Theoretische Physik , Leibniz Universität Hannover, Appelstr. 2, D-30167, Hannover, Germany

Faraday patterns can be induced in Bose-Einstein condensates by a periodic modulation of the system nonlinearity. We show that these patterns are remarkably different in dipolar gases with a roton-maxon excitation spectrum. Whereas for non-dipolar gases the pattern size decreases monotonously with the driving frequency, patterns in dipolar gases present, even for shallow roton minima, a highly non trivial frequency dependence characterized by abrupt pattern size transitions, which are especially pronounced when the dipolar interaction is modulated. Faraday patterns constitute hence an optimal tool for revealing the onset of the roton minimum, a major key feature of dipolar gases.

The formation of Faraday patterns in driven systems is a general phenomenon occurring in scenarios ranging from hydrodynamics and non-linear optics, to liquid crystals and chemical reactions [1]. Faraday patterns may be observed in Bose-Einstein condensates (BECs) by modulating the nonlinearity arising from the interatomic interactions [2] either by time-dependent Feshbach resonances [3] or by a time-dependent confinement. The latter method has been recently used for realizing these patterns in BECs [4]. Faraday patterns offer important insights about elementary excitations in BECs since the pattern size is determined by the Bogoliubov mode resonant with half of the driving frequency. For usual short-range interacting BECs the energy of elementary excitations grows monotonously as a function of their corresponding momenta. As a result, the pattern size decreases monotonously with the driving frequency.

Recent experiments on atoms with large magnetic moments [5, 6], polar molecules [7, 8], spinor Bose-Einstein condensates (BECs) [9], and optical lattices [10] are opening the rapidly-developing area of dipolar gases. In these gases, the dipole-dipole interactions (DDIs) play a significant or even dominant role compared to the short-range interactions (SRIs). Dipolar BECs present a wealth of new physics [11, 12, 13, 14] due to the long-range and anisotropic character of the DDI. A major salient difference between non-dipolar and dipolar BECs is provided by the dispersion of elementary excitations, which, due to the momentum dependence of the DDI, may show a roton-maxon character [14], similar to that encountered in Helium physics [15]. This key feature of dipolar gases may significantly influence, for deep roton minima, the BEC properties at finite temperatures [16] and even the BEC stability [17]. The roton minimum has not yet been observed experimentally, and it remains still an open question how to probe easily the onset of rotonization.

In this Letter, we show that pattern formation is crucially modified in dipolar BECs with a roton-maxon spectrum. Remarkably, contrary to many pattern forming systems, including non-dipolar BECs, the first unstable mode does not necessarily determine the emerging pattern, which may be dominated by harmonics of the driv-

ing frequency with energies close to the roton minimum. As a result of that and of the multi-valued character of the roton-maxon spectrum the pattern size presents a highly non trivial dependence with the driving frequency characterized even for shallow roton minima by abrupt transitions in the pattern size. These transitions, which are especially pronounced when the DDI is modulated, may be employed to reveal easily the appearance of a roton-minimum in experiments on dipolar BECs.

We consider a BEC of N particles with mass m and electric dipole d (the results are equally valid for magnetic dipoles) oriented in the z -direction by a sufficiently large external field. The dipoles interact via a dipole-dipole potential: $V_d(\vec{r}) = d^2(1 - 3\cos^2(\theta))/r^3$, where θ is the angle formed by the vector joining the interacting particles and the dipole orientation. We assume a strong harmonic confinement $V(z) = m\omega_z^2 z^2/2$ along the z -direction, whereas for simplicity of our discussion we consider no xy trapping. At sufficiently low temperatures the BEC wavefunction $\Psi(\vec{r})$ is given by the non-local non-linear Schrödinger equation (NLSE):

$$i\hbar\frac{\partial}{\partial t}\Psi(\vec{r}) = \left[\hat{H}_0 + \int d^3r' U(\vec{r} - \vec{r}') |\Psi(\vec{r}')|^2 \right] \Psi(\vec{r}), \quad (1)$$

where $\hat{H}_0 = -\hbar^2\nabla^2/2m + V(z)$ and $U(\vec{r}) = g\delta(\vec{r}) + V_d(\vec{r} - \vec{r}')$, with $g = 4\pi\hbar^2 a/m$, where a the s -wave scattering length (we consider in the following $a < 0$), and m the particle mass. If the chemical potential (below introduced) $\mu_{2d} \ll \hbar\omega_z$, the system can be considered “frozen” into the ground state $\phi_0(z)$ of V and hence the BEC wave function factorizes as $\Psi(\vec{r}) = \psi(\vec{\rho})\phi_0(z)$. Employing this factorization, the convolution theorem, the Fourier transform of the dipole-potential and integrating over the z direction, we arrive at the 2D NLSE [18]:

$$i\hbar\frac{\partial}{\partial t}\psi(\vec{\rho}) = \left[-\frac{\hbar^2}{2m}\nabla^2 + g_{2d}|\psi(\vec{\rho})|^2 + \frac{4\pi}{3}\beta g_{2d} \int \frac{d^2k}{(2\pi)^2} e^{i\vec{k}\cdot\vec{\rho}} \tilde{n}(\vec{k}) h_{2d} \left(\frac{kl_z}{\sqrt{2}} \right) \right] \psi(\vec{\rho}), \quad (2)$$

where \vec{k} is the xy -momentum, $l_z \equiv \sqrt{\hbar/m\omega_z}$ is the oscillator length, $g_{2d} \equiv g/\sqrt{2\pi}l_z$ is the 2D short-range coupling constant, $\tilde{n}(\vec{k})$ is the Fourier transform of $|\psi(\vec{\rho})|^2$,

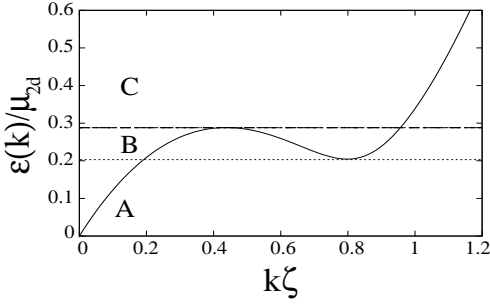


Figure 1: Dispersion of a 2D homogeneous BEC of ^{52}Cr with $a = -0.54\text{nm}$ ($\beta = -0.375$), a 3D density $\bar{n}_{2d}/\sqrt{2\pi}l_z = 10^{14}\text{cm}^{-3}$, $\hbar\omega_z = \mu_{2d}/2$, and $\zeta = \hbar/\sqrt{2m\mu_{2d}} = 0.59\mu\text{m}$.

and $h_{2d}(\vec{k}) = 2 - 3\sqrt{\pi}ke^{k^2}\text{erfc}(k)$, with $\text{erfc}(k)$ the complementary error function. The parameter $\beta = d^2/g$ characterizes the DDI strength compared to the SRI.

The homogeneous solution of (2) is $\psi(\vec{\rho}, t) = \sqrt{\bar{n}_{2d}}\exp[-i\mu_{2d}t/\hbar]$, with n_{2d} the 2D density, and $\mu_{2d} = g_{2d}n_{2d}(1 + 8\pi\beta/3)$ the chemical potential. The elementary excitations of the homogeneous 2D BEC are plane waves with 2D wave number \vec{k} and dispersion [19]

$$\epsilon(k)^2 = T(k) \left[T(k) + 2g_{2d}n_{2d} \left[1 + \frac{4\pi\beta}{3} h_{2d} \left(\frac{kl_z}{\sqrt{2}} \right) \right] \right] \quad (3)$$

where $T(k) = \hbar^2 k^2/2m$ is the kinetic energy. If $\beta = 0$ and since $a < 0$ then $\epsilon(k \rightarrow 0)^2 < 0$ and phonon instability occurs, followed by the well-known collapse for attractive short-range interacting BECs. This instability is prevented for sufficiently large DDI such that $g + 8\pi d^2/3 > 0$. At moderate d values, and due to the k -dependence of the DDI (h_{2d} function), $\epsilon(k)$ may develop a roton-like minimum for intermediate k values (see Fig. 1). The roton-maxon spectrum constitutes one of the most relevant novel features in dipolar gases. We show below that this roton minimum may be easily probed even for shallow roton minima by modulating the system nonlinearity.

We consider a modulation $a(t) = a_0[1 + 2\alpha \cos(2\omega t)]$ about its mean a_0 , where α is the modulation amplitude and 2ω is the driving frequency. The homogeneous 2D solution is $\psi_H(\vec{\rho}, t) = \sqrt{\bar{n}_{2d}}\exp[-i(t + \frac{\gamma}{\omega} \sin(2\omega t))\mu_{2d}/\hbar]$, with $\gamma = \alpha/(1 + 8\pi\beta/3)$. The driving may induce a dynamical instability breaking the translational symmetry. This destabilization is best studied with an ansatz $\psi(\vec{\rho}, t) = \psi_H(t)[1 + w(t) \cos(\vec{k} \cdot \vec{\rho})]$, where $w(t)$ is the complex perturbation amplitude. Inserting this ansatz into (2) we obtain a Mathieu equation for $u = \text{Re}(w)$:

$$\frac{d^2 u}{dt^2} + \frac{1}{\hbar^2} [\epsilon(k)^2 + 2b(\omega, k, \alpha)(\hbar\omega)^2 \cos(2\omega t)] u = 0, \quad (4)$$

where $b(\omega, k, \alpha) \equiv 2\alpha|g_{2d}|n_{2d}T(k)/(\hbar\omega)^2$, where g_{2d} is calculated from the mean a_0 . Following Floquet Theorem, the solutions of (4) are of the form $u(t) = c(t) \exp \sigma t$, where $c(t) = c(t + 2\pi/\omega)$ and $\sigma(k, \omega, \alpha)$ is the so-called

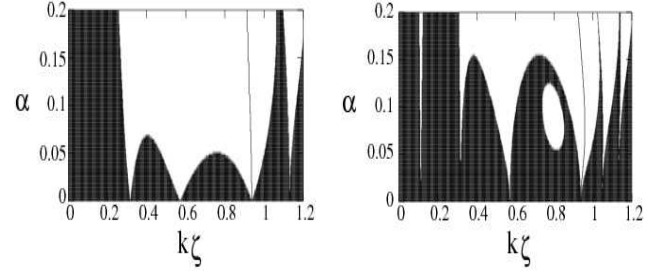


Figure 2: Stability diagram (dark regions are stable) for the parameters of Fig. 1 as a function of α and k . (Left) $\hbar\omega/\mu = 0.268$ (regime B). (Right) $\hbar\omega/\mu = 0.134$ (regime A). The most unstable modes are indicated by a solid line.

Floquet exponent. If $\text{Re}(\sigma) > 0$ the homogeneous BEC is dynamically unstable against the formation of Faraday patterns, whose typical wavelength is dominated by the most unstable mode (that with the largest $\text{Re}(\sigma) > 0$). For vanishing modulation the system becomes unstable at the parametric resonances $\epsilon(k) = n\hbar\omega$ ($n = 1, 2, \dots$).

BECs with repulsive short-range interactions exhibit a spectrum $\epsilon(k)^2 = T(k)[T(k) + 2g_{2d}n_{2d}]$, characterized by phonon-like excitations at low k and single-particle excitations at large k . For any given driving frequency the most unstable mode is always provided by the first resonance $\epsilon(k) = \hbar\omega$, and hence $k = \epsilon^{-1}(\hbar\omega)$ determines the typical inverse size of the Faraday pattern [20]. As a consequence a larger driving frequency leads to a pattern of smaller size, as shown in recent experiments [2]. In the following we show that the physics of Faraday patterns is remarkably much richer and involved in dipolar BECs.

As mentioned above, for intermediate d values $\epsilon(k)$ shows a roton minimum (with energy $\hbar\omega_r$) and a maxon maximum ($\hbar\omega_m$). Hence, as a function of the modulation frequency 2ω we may distinguish three driving regimes: (A) $\omega < \omega_r$, (B) $\omega_r \leq \omega \leq \omega_m$ and (C) $\omega > \omega_m$ (see Fig. 1). The latter regime is relatively uninteresting, since, as for non-dipolar BECs, the spectrum is uni-valued and the most unstable mode is provided by $\epsilon(k) = \hbar\omega$. The regime B on the contrary is multi-valued, and the condition $\epsilon(k) = \hbar\omega$ is satisfied by a triplet $k_1 < k_2 < k_3$. These three resonant momenta lead to three instability tongues for growing modulation amplitude α (Fig. 2(a)). Hill's solution method [20, 21] provides that for the lowest resonance $\epsilon(k) = \hbar\omega$, the Floquet exponent may be approximated for small b as $\sigma_1 = b(\omega, k, \alpha)/2 \propto k^2/(\hbar\omega)^2$. Hence the most unstable mode in regime B is always given by the largest momentum k_3 , which dominates the Faraday pattern formation.

For regimes B and C the Faraday pattern is, as for non-dipolar BECs, provided by $\epsilon(k) = \hbar\omega$. The situation is remarkably different for regime A. The latter is better understood by considering the ratio σ_2/σ_1 between the Floquet exponents for the second ($\epsilon(k) = 2\hbar\omega$) and the first ($\epsilon(k) = \hbar\omega$) resonance condition. This ratio may be

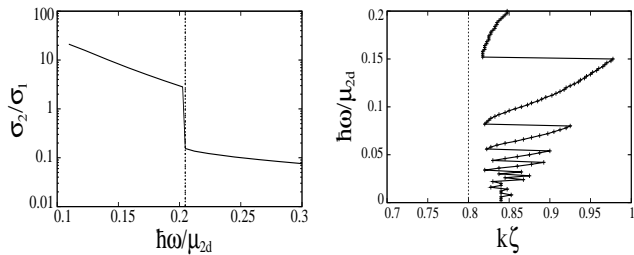


Figure 3: (Left) Ratio between the Floquet exponent σ_1 for $\epsilon = \hbar\omega$ and σ_2 for $\epsilon = 2\hbar\omega$. (Right) Most unstable k as a function of ω . We use the same parameters as for Fig. 1. The dashed line indicates the roton frequency or momentum.

obtained by using again Hill's solution method [20, 21]:

$$\frac{\sigma_2}{\sigma_1} = \frac{\sqrt{5}\alpha}{12(8\pi|\beta|/3-1)} \left(\frac{\mu_{2d}}{\hbar\omega}\right)^2 \zeta^2 \frac{[\epsilon^{-1}(2\hbar\omega)]^4}{[\epsilon^{-1}(\hbar\omega)]^2} \quad (5)$$

where $\zeta = \hbar/\sqrt{2m\mu_{2d}}$ is the healing length. Not surprisingly, the first resonance dominates for $\alpha \rightarrow 0$. However, contrary to the short-range interacting case, for α surpassing a very small ω -dependent critical α the situation changes completely. Fig. 3(a) depicts the ratio σ_2/σ_1 as a function of ω for a small $\alpha = 0.04$. Note that for $\omega > \omega_r$, $\sigma_2 < \sigma_1$, and as expected, for regimes B and C the instability is dominated by the resonance $\epsilon(k) = \hbar\omega$. On the contrary for $\omega < \omega_r$, $\sigma_2 > \sigma_1$ even for such a small value of α , and hence the lowest resonance is not any more the most unstable one. This surprising result is a direct consequence of the non-monotonous character of the roton-maxon dispersion law.

Our numerical Floquet analysis shows indeed (see Fig. 3(b)) that for $\alpha > \alpha_{cr}$ (for the parameters of Figs. 2 $\alpha_{cr} \simeq 0.027$) the most unstable mode for all driving frequencies within the regime A is given by the largest momenta k compatible with the first harmonic $\epsilon(k) = n\hbar\omega$ lying in the regime B (or, if none, the first lying in regime C). This has important consequences for the wavenumber selection as a function of the driving ω , which, as shown in Fig. 3(b), is remarkably different than that for the non-dipolar case. The pattern size does not decrease monotonously with growing ω , but on the contrary oscillates in the vicinity of the roton momentum, presenting abrupt changes of the pattern size at specific driving frequencies. These oscillations are the result of the subsequent destabilization of higher harmonics in regime B.

This distorted wave number selection is directly mirrored into the spatial form of the corresponding Faraday patterns. We have studied the dynamical instability induced by the modulation and the corresponding Faraday patterns by simulating Eq. (2) numerically with periodic boundary conditions and an overimposed random noise provided by a tiny random local phase ($< 10^{-3}\pi$) on the homogeneous solution. Our direct numerical calculations is in excellent agreement with our Floquet analysis.

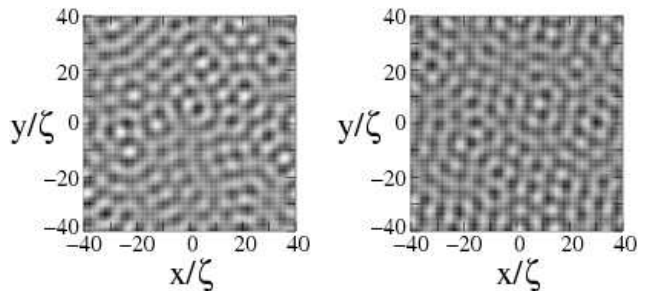


Figure 4: Faraday patterns for $\hbar\omega/\mu = 0.268$ at $t = 40.6$ ms (left) and $\hbar\omega/\mu = 0.134$ at $t = 93.2$ ms (right), and the same parameters as in Fig. 1.

Fig. 4(a) depicts the case of a frequency $\omega_r < \omega_0 < \omega_m$, where as expected the Faraday pattern is indeed given by the largest resonant momentum. In Fig. 4(b) we consider $\omega = \omega_0/2$ which is within the regime A. Strikingly, due to the discussed selection of higher harmonics, the Faraday pattern is basically the same as for a double driving frequency ω_0 . This quasi-insensitivity becomes quantitatively evident after Fourier transforming the pattern.

In the previous discussion we considered the modulation of the s -wave scattering length $a(t)$. A dipolar BEC offers, however, an additional novel way of modifying the system nonlinearity by a time-dependent DDI. This may be achieved by modulating slightly the intensity of the polarizing field (e.g. the electric field orienting a polar molecule) or by introducing a slight precession of the direction of the external field (e.g. by additional transversal magnetic fields in the case of atomic dipoles). In the following we show that the Faraday patterns obtained by means of a modulated DDI differ very significantly from those obtained by modulating $a(t)$.

We consider a temporal modulation of the DDI $d^2 = g\beta(t)$, with $\beta(t) = \bar{\beta}[1+2\alpha\cos(2\omega t)]$ about its mean value $\bar{\beta}$. Following a similar procedure as that discussed above for the case of modulated $a(t)$, we obtain the Mathieu equation for the real part of the perturbation amplitude. This equation is of the same form as Eq. (4) but with

$$b(\omega, k, \alpha) = \frac{8\pi\alpha|\bar{\beta}g_{2d}|n_{2d}}{3(\hbar\omega)^2} T(k)h_{2d} \left(\frac{kl_z}{\sqrt{2}}\right). \quad (6)$$

The modified k -dependence of $b(\omega, k, \alpha)$ has crucial consequences for the formation of Faraday patterns. Similarly as above we may obtain from Hill's solution method the Floquet exponent for the first resonance $\epsilon(k) = \hbar\omega$, $\sigma_1 \propto k^2h_{2d}(kl_z/\sqrt{2})$. This leads to a remarkably different selection rule for ω values within the regime B. Contrary to the case of modulated $a(t)$, it is the intermediate momentum k_2 and not the largest one k_3 the most unstable within regime B. This leads to a remarkably abrupt change in the Faraday pattern size in the vicinity of ω_m [22]. In addition, and similar to the case of modulated $a(t)$, driving with $\omega < \omega_r$ may be dominated by

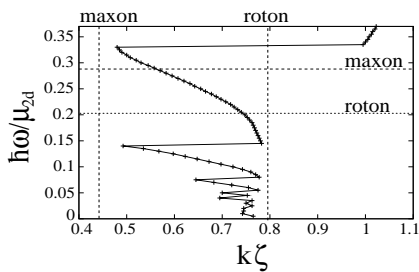


Figure 5: Most unstable k as a function of ω for modulated $\beta(t)$, $\alpha = 0.12$, and the same parameters as for Fig. 1. We indicate the roton and maxon frequencies and momenta.

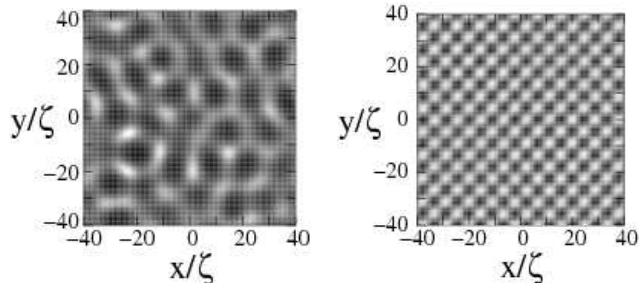


Figure 6: Faraday patterns for $\hbar\omega/\mu = 0.32$ at $t = 116.7$ ms (left) and $\hbar\omega/\mu = 0.34$ at $t = 405.1$ ms (right), and the same parameters as in Fig. 5.

higher harmonics. Fig. 5 shows the most unstable k as a function of ω for a typical case of modulated $\beta(t)$. Note not only the above mentioned abrupt jump in the vicinity of ω_m but also at other ω values within the regime A. As for the case of modulated $a(t)$ these jumps represent abrupt transitions in the Faraday pattern size, which are certainly much more marked than for the modulated a case. Figs. 6 show the abrupt change in the patterns for two driving frequencies right below and above the transition close to ω_m [22].

In our calculations we have assumed for simplicity no trapping on the xy plane. An harmonic xy -confinement (with frequency ω_\perp) leads to a finite momentum cut-off $k_c = \sqrt{m\omega_\perp/\hbar}$. In a good approximation all features in the excitation spectrum with momenta $k \gg k_c$ are not affected by the inhomogeneous trapping. For typical roton momenta $k\xi \simeq 0.5$ and $\xi \simeq 0.6\mu\text{m}$ in our figures, $k \gg k_c$ demands for ^{52}Cr a transversal frequency $\omega_\perp < 130\text{Hz}$, which can be considered a typical experimental condition. Finally, we stress that Faraday patterns are a transient

phenomenon, and that for the case discussed here ($a < 0$) pattern formation is followed by collapse (and consequent violation of the two-dimensional condition).

In summary, the physics of Faraday patterns is largely modified in dipolar BECs in the presence of even shallow roton minima. Whereas in non-dipolar BECs the Faraday pattern size decreases monotonously with the driving frequency 2ω , in dipolar BECs the patterns show a ω -dependence characterized by abrupt changes in the pattern size, which are especially remarkable when the dipole itself is modulated. Faraday patterns constitute hence an excellent tool to probe the onset of rotonization in on-going experiments with dipolar condensates.

This work was supported by the DFG (SFB407, QUEST), and the ESF (EUROQUASAR).

-
- [1] M. C. Cross and P. C. Hohenberg, *Rev. Mod. Phys.* **65**, 851 (1993).
 - [2] K Staliunas *et al.*, *Phys. Rev. Lett.* **89**, 210406 (2002).
 - [3] S. Inouye *et al.*, *Nature* **392**, 151 (1998).
 - [4] P. Engels *et al.*, *Phys. Rev. Lett.* **98**, 095301 (2007).
 - [5] A. Griesmaier *et al.*, *Phys. Rev. Lett.* **94**, 160401 (2005).
 - [6] Q. Beaufils *et al.*, *Phys. Rev. A* **77**, 061601 (R) (2008).
 - [7] S. Ospelkaus *et al.*, *Nature Phys.* **04**, 622 (2008).
 - [8] J. Deiglmayr *et al.*, *Phys. Rev. Lett.* **101**, 133004 (2008).
 - [9] M. Vengalattore *et al.*, *Phys. Rev. Lett.* **100**, 170403 (2008).
 - [10] M. Fattori *et al.*, *Phys. Rev. Lett.* **101**, 190405 (2008).
 - [11] S. Yi and L. You, *Phys. Rev. A* **61**, 041604 (2000).
 - [12] K. Góral, K. Rzȃżewski, and T. Pfau, *Phys. Rev. A* **61**, 051601 (2000).
 - [13] L. Santos *et al.*, *Phys. Rev. Lett.* **85**, 1791 (2000).
 - [14] L. Santos, G. V. Shlyapnikov, and M. Lewenstein, *Phys. Rev. Lett.* **90**, 250403 (2003).
 - [15] R. P. Feynman, *Phys. Rev.* **94**, 262 (1954).
 - [16] D. W. Wang and E. Demler, arXiv:0812.1838.
 - [17] S. Komineas and N. R. Cooper, *Phys. Rev. A* **75**, 023623 (2007); S. Ronen, D. C. E. Bortolotti, and J. L. Bohn, *Phys. Rev. Lett.* **98**, 030406 (2007).
 - [18] P. Pedri and L. Santos, *Phys. Rev. Lett.* **95**, 200404 (2005).
 - [19] U. Fischer, *Phys. Rev. A* **73**, 031602(R) (2006).
 - [20] A. L. Nicolin, R. Carretero-González, P. G. Kevrekidis, *Phys. Rev. A* **76**, 063609 (2007).
 - [21] A. Nicolin, PhD Thesis, Copenhagen 2008.
 - [22] For finite α the transitions slightly shift from their values at $\alpha \simeq 0$.